Iranian Journal of Science and Technology, Transactions of Civil Engineering (2024) 48:1329–1352
https://doi.org/10.1007/s40996-023-01226-3

RESEARCH PAPER

Examination of mechanical, permeability, and durability properties of sustainable lightweight concrete composites with natural perlite aggregate

H. Alperen Bulut[1]

Received: 21 April 2023 / Accepted: 26 August 2023 / Published online: 13 September 2023

Abstract

This article presents the outcomes of a comprehensive study utilizing all-natural perlite in producing lightweight aggregate concrete composites and investigating the mechanical, permeability, and durability properties. With this aim, lightweight concrete composites were produced using 10%, 20%, 30%, 40%, 50%, 75% and 100% of natural perlite aggregate in concrete production. In addition to fresh density, compressive strength, ultrasonic pulse velocity (UPV), dynamic modulus of elasticity, capillary absorption, electrical resistivity, acid and sulfate attack tests were carried out on 28–56–90-day-ϖold concretes. Accordingly, the highest compressive strength value was obtained after 90 days using 10% natural perlite (62.42 MPa for NP10/90). In terms of UPV values, concretes with natural perlite were able to produce good or excellent class concretes. The experimental results indicated that the increase in the dynamic modulus of elasticity of concretes cured for 90 days (35 GPa for NP100/90) can be up to 14% compared to concretes cured for 28 days (30.7 GPa for NP100/28). Capillary absorption coefficients decreased in all concretes at advanced ages. The electrical resistivity value of concrete with 100% natural perlite (139.75 kΩ-m for NP100/90) was 140% higher than the control concrete (58.14 kΩ-m for C/90). It was observed that insulating concrete could be produced with an increase in the use of natural perlite at advanced ages. It was determined that concretes with 75% and 100% natural perlite exhibited high resistance against acid and sulfate attacks. The 30% perlite ratio was the critical ratio against aggressive solutions. In line with the aim of the study, it has been proved that lightweight concretes with a high natural perlite dosage can be produced in terms of permeability and durability properties without compromising mechanical strength.

✉ H. Alperen Bulut
habulut@erzincan.edu.tr

[1] Engineering and Architecture Faculty, Department of Civil Engineering, Erzincan Binali Yıldırım University, 24002 Erzincan, Turkey

Graphical abstract

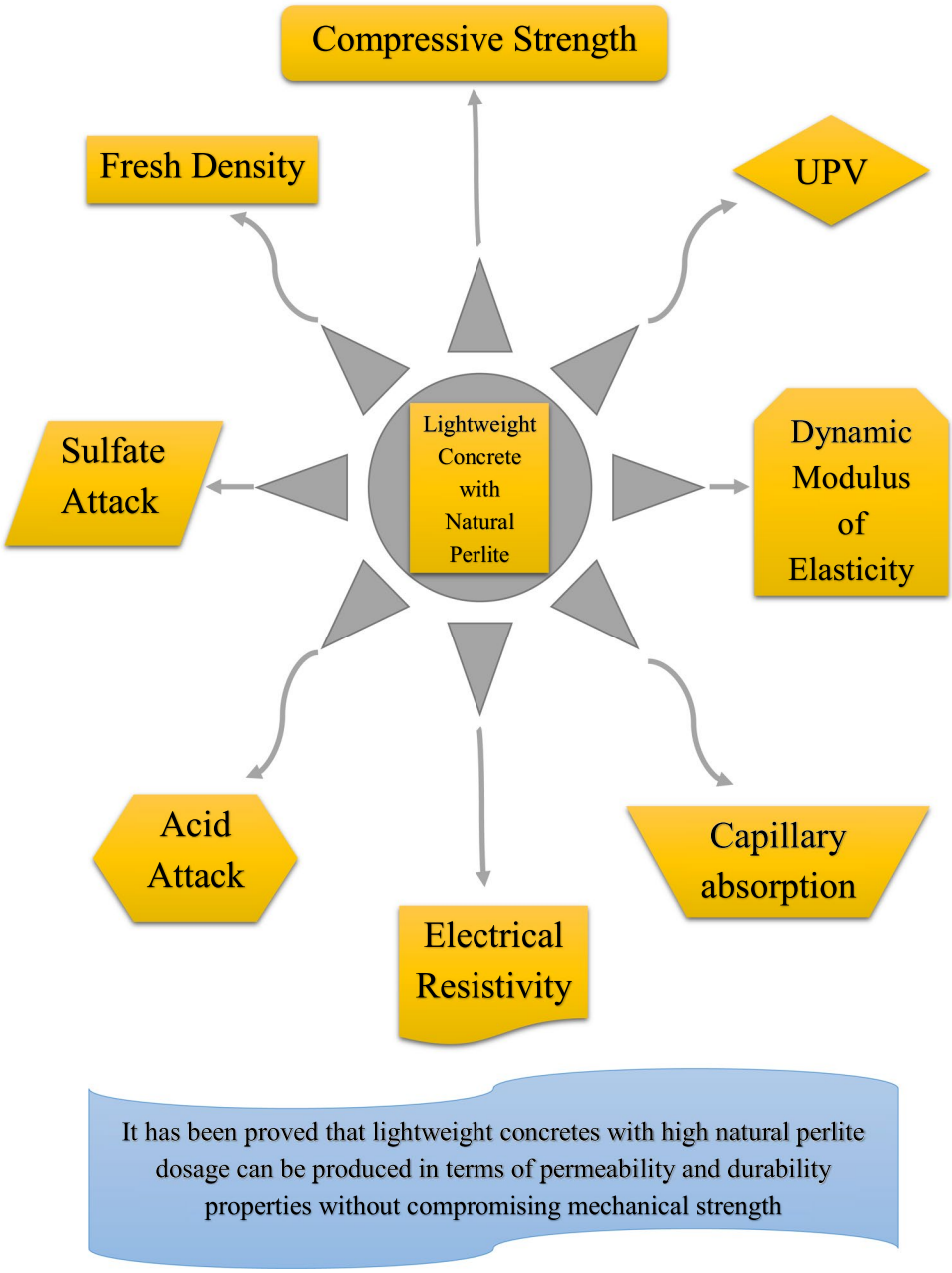

Keywords Lightweight concrete · Perlite · Mechanical properties · Permeability · Acid attack · Sulfate attack

1 Introduction

The increase in urbanization and industrialization over the last 200 years has resulted in dramatic growth in both material use and energy consumption (Krausmann et al. 2009). While this increase results from human actions, the damage caused to the environment by the construction industry through unhealthy practices has been significant (Ortiz et al. 2009). In this context, it has been stated that the construction industry is responsible for 8% of total annual carbon dioxide (CO_2) production (Arrigoni et al. 2020) and 40% of total energy consumption (Zhao et al. 2020). If no action is taken, it is predicted that the total CO_2 production from the construction sector could increase to 25% by 2050 (Snellings 2016). In order to overcome these challenges, the sustainable utilization of high-performance composite materials is

recommended and implemented (Gencel et al. 2022). For example, Esfandiari and Heidari (2021) studied the behavior of high-performance concrete composites with optimum percentages of steel fibers, metallic fibers, polypropylene fibers and pozzolanic materials (fly ash and microsilica) at different ratios in the production of concrete and made recommendations by examining the behavior of high-performance concrete composites with optimum percentages under different loads.

Many properties of aggregates such as shape, roughness, specific gravity, chemical and mineral composition, strength and pore structure depend on the properties of the parent rock (Swamy and Tanikawa 1993). It is recognized that aggregates, which constitute approximately 75% of concrete, significantly affect the performance of concrete (Akyuncu and Sanliturk 2021). Concrete, the most widely used building material, is expected to have increasingly improved properties such as low density and low cost, while maintaining generally superior mechanical and durability properties (Yu et al. 2016; Hanif et al. 2017; Chinchillas-Chinchillas et al. 2019). Lightweight concrete, which is typically obtained by adding lightweight aggregate to concrete, not only reduces the self-weight of structures, but also provides savings in terms of reinforcement, transportation, foundation cost and high energy efficiency with reduced concrete density (Zhang et al. 2015, 2016; Siwowski and Rajchel 2019; Sahoo et al. 2020; Burbano-Garcia et al. 2021; Wang et al. 2022). Considering that sustainable development is a critical global issue in the present day, energy savings and reduction of environmental impact can be implemented through the use of lightweight concrete (Leong et al. 2020). In order to produce lightweight concrete with the desired unit weight and adequate mechanical properties, it is significant to specify and employ suitable lightweight aggregates. Natural lightweight aggregates frequently utilized in lightweight concrete production are recognized as pumice, shale ceramsite, scoria, perlite, and coconut shale (Adhikary et al. 2022). Materials such as expanded clay, expanded shale, expanded glass, expanded polystyrene, waste/recycled plastic, waste/recycled rubber and fly ash are commonly used as artificial lightweight aggregates (Aslam et al. 2016).

Due to its low density, perlite is a suitable material for producing lightweight concrete (Sengul et al. 2011). Perlite is defined as a glassy amorphous volcanic rock that can expand up to 35 times its original volume when heated to 1100 °C (Lanzón and García-Ruiz 2008). Perlite has a porous and rough structure, which contributes to its light weight (Işıkdağ 2015). Due to its glassy structure and high silicon dioxide (SiO_2) and aluminum oxide (Al_2O_3) content, perlite is also classified as an artificial pozzolanic material (Rashad 2016). It has been reported that concretes with perlite exhibit good resistance to durability problems such as freeze–thaw and fire and provide improved acoustic comfort (Abdul et al. 2019; Jia and Li 2021; Baskar et al. 2022). Perlite is utilized as plaster and insulation material in the construction industry as well as in the agriculture, food, and pharmaceutical sectors (Topçu and Işıkdağ 2007; Diamanti et al. 2013). However, perlite is not widely recognized in concrete yet.

In the literature, there are studies on using expanded perlite as aggregate in mortar/concrete. A study on the thermal conductivity and compressive strength of concrete with mineral admixed expanded perlite aggregate (Demirboğa and Gül 2003), it was reported that the thermal conductivity of lightweight concretes decreased up to 13%. Sengul et al. (2011) investigated the effects of expanded perlite on the mechanical properties and thermal conductivity of lightweight concrete. They emphasized that thermal conductivity increased significantly with the inclusion of perlite and a strong relationship was obtained between thermal conductivity and unit weight. A study investigating the mechanical and thermophysical properties of lightweight aggregate concretes (Oktay et al. 2015) revealed improved insulation properties of expanded perlite aggregate composites. Akyuncu and Sanliturk (2021) investigated the physical and mechanical properties of mortars produced with polymer-coated expanded perlite aggregate. As a result, mortar samples with better thermal insulation properties were obtained with decreasing thermal conductivity values.

In a study on the self-healing of alkali-active mortars with expanded perlite aggregate (Polat 2022), it was reported that bacterial cells were able to sporulate directly on the expanded perlite aggregate, greatly improving the crack closure rate of the specimens up to 100%. Wang et al. (2022) reported that the utilization of expanded perlite yielded positive results in the production of ultra-high strength lightweight concrete. In another study (Gencel et al. 2022), which investigated the properties of lightweight foam concretes containing expanded perlite and glass sand, it was stated that the use of expanded perlite potentially improves the insulation properties of foam concrete due to the high porosity of expanded perlite compared to glass sand. Pasupathy et al. (2022) conducted an experimental study to improve the properties of foam concrete 3D printers by utilizing porous aggregates. Accordingly, it was proven that combining expanded perlite and foam significantly improved the fresh and hardened properties of the lightweight concrete produced.

Although studies on the utilization of expanded perlite in lightweight concrete technology have been reported, there are minimal studies in which natural perlite is directly used as an aggregate in lightweight concrete without any process (Kalpana and Tayu 2020; Chihaoui et al. 2022; Ragul et al. 2022). In this context, more elaborate studies

are necessary to obtain valuable conclusions. The main objective of this study is to present a new and sustainable evaluation of the use of all-natural perlite instead of conventional aggregate for the preparation of lightweight aggregate composites by investigating the mechanical, permeability, and durability properties of these composites. This study also aims to increase the dosage of natural perlite as much as possible to obtain the best dosage in terms of permeability and durability properties without compromising mechanical strength. For this purpose, lightweight concrete composites were produced by using 10%, 20%, 30%, 40%, 50%, 75%, and 100% of natural perlite aggregate instead of fine and coarse aggregates. In addition to fresh density, mechanical properties (compressive strength, UPV, dynamic modulus of elasticity), permeability properties (capillary water absorption, electrical resistivity), and durability properties (acid attack, sulfate attack) were extensively investigated on 28–56–90-day-old concretes. Compared to conventional concrete, lightweight concretes produced with natural perlite may have benefits such as less destruction of natural resources, more environmentally friendly, more sustainable, and superior engineering properties. This study provides a reference on the properties of lightweight concrete composites with natural perlite aggregate. It can be defined as research in accordance with the concept of sustainable development.

2 Experimental methodology

2.1 Materials

CEM I 42.5 *R* type Portland cement was used in the study. The specific properties of this cement are shown in Table 1. Crushed stone of limestone origin in two grades (4/8 mm and 8/16 mm) as a coarse aggregate (specific gravity; 2.68 g/cm^3) and natural river sand in three grades (0/1 mm, 1/2 mm and 2/4 mm) as a fine aggregate (specific gravity; 2.66 g/cm^3) have been used in the production of control concretes. Lightweight concretes were also produced with natural perlite aggregate of the same gradation.

Polycarboxylate ether-based high-performance superplasticizer (SP) (new generation) additive was utilized as a chemical additive in the study. The properties of the chemical additive obtained from the manufacturer are shown in Table 2

Granulated, pumice, concentric, fibrous, phenocrystalline and sandy natural perlite types are used. All of the natural perlite used in the study was supplied by the ERPER company operating in Erzincan/TR, which has an annual perlite production capacity of 384,000 tons. The figure of natural perlite used in production is given in Fig. 1.

Table 1 Properties of cement

CEM I 42.5 R	
Chemical compositions (%)	
SiO_2	19.21
Al_2O_3	4.87
Fe_2O_3	3.12
CaO	64.29
MgO	2.47
SO_3	2.85
Na_2O	0.31
K_2O	0.70
CI^-	0.01
Loss on ignition	2.84
Insoluble residue	0.72
Physical characteristics	
Residue on a 32 micron sieve	7.38
Specific gravity	3.12
Specific surface (cm^2/g)	3441
Beginning of setting	2 h-33 min
End of setting	3 h-29 min
Volume expansion (mm)	1.0
Compressive strength (MPa)	
2nd day	26.8
28th day	53.8

Table 2 Product and technical data of the superplasticizer

Properties	MasterGlenium 51
Chemical base	Polycarboxylate ether
Appearance	Brownish liquid
Density (at + 20 °C) (gr/cm^3)	1.082–1.142
pH value	6–7
Alkali content (w/w, %)	≤ 3
Soluble in water chloride ion content (by mass, %)	≤ 0.10

The properties of natural perlite aggregates obtained from the manufacturer are shown in Table 3. The specific gravity of natural perlite used at different ratios in concretes is 2.015 g/cm^3.

SEM images showing the internal structure of natural perlite are given in Figs. 2 and 3. As seen in Figs. 2 and 3, the structure of natural perlite consists of a limited quantity of air and very thin and many capillary spaces with filigree lamellar widths (Schumacher et al. 2020). Particularly in Fig. 3, portlandite crystals and C–S–H phase were observed in the microstructure of perlite aggregate. Although these particles have a highly developed surface, they could not be labeled as smooth. Similar results were

Fig. 1 The figure of natural perlite aggregates

Table 3 Properties of natural perlite aggregates

Natural perlite Aggregates	
Mineral compositions (%)	
SiO_2	73.70
Al_2O_3	12.32
Fe_2O_3	1.08
CaO	0.69
MgO	0.04
TiO_2	0.032
Na_2O	3.89
K_2O	4.19
FeO	0.33
MnO	0.069
P_2O_3	0.008
Physical characteristics	
Bulk density (g/cm^3)	2.03–2.16
Water absorption 24 h (% by weight)	6% max
Consistency water requirement	18%
Los Angeles abrasion	67%
Strength index 7-days	78%
Strength index 28-days	80%

obtained by Barnat-Hunek et al. (2021). In addition, it can be noticed that natural perlite has a porous and flaky structure, irregularly shaped grains of different sizes, rough, broken, sharp and irregular edges.

Especially the surface morphology of natural perlite was similar to other studies (Aghabeyk et al. 2022).

Mineral composition analysis was carried out to prove the pozzolanic reaction properties of perlite. Accordingly, the natural perlites employed in the study were analyzed for compliance with the requirements specified in ASTM C 618 (2023), the standard specification for natural pozzolans. In Table 4, the results of the analysis are given in comparison with the standard.

As a result, the chemical composition of perlites exhibiting siliceous structure (Table 3), their compliance with ASTM C 618 (2023), the standard specification for natural pozzolans (Table 4), and previous studies on pozzolanic properties of perlites (Urhan 1987; Demirboğa et al. 2001; Yu et al. 2003; Erdem et al. 2007; Karein et al. 2018; Esfandiari and Loghmani 2019; Junaid et al. 2022), prove in many aspects that perlites have certain pozzolanic properties.

2.2 Concrete mix design

The parameter selected within the scope of the study was natural perlite. The replacement percentages of all parameters (i.e., the parameter) were 10%, 20%, 30%, 40%, 50%, 75% and 100%, respectively, of the crushed stone and natural river sand by volume. However, no natural perlite was added to the control mixes. In the coding, the abbreviation of natural perlite was indicated by their first letters, the natural perlite ratios were represented by the numbers after the letters (without using the % sign), and the numbers designated the test days after the '/' sign. For example, NP30/56 represented the mixture containing 30% natural perlite and was tested on day 56. The control concretes were denoted by *C*. Throughout the production process, the cement dosage, water/cement ratio, and dosage rate of the superplasticizer were kept constant at 450 kg/m^3, 0.45, and 0.7%, respectively. The concrete mix design prepared for the study is presented in Table 5. The codes in the table omitted the numbers representing the day of the hardened concrete tests.

2.3 Testing of concretes

During the concrete production, a coarse aggregate and cement were first mixed in a laboratory pan mixer with a capacity of 35 l and a vessel velocity of 25 rpm for 30 s. A fine aggregate, water, and a superplasticizer were then incorporated into the mixer and mixed for 6 min. After recording the fresh density properties for each batch, the batches were placed in plastic cube molds with compaction, kept in the mold for 24 h, and cured in water until the testing day.

The determination of fresh density for the concrete specimens was conducted following the guidelines specified in the TS EN 12350-6 (2019) standard. Compressive strength tests were performed at the end of the 28th, 56th, and 90th day of curing according to the TS EN 12390-3 (2019) standard on all cube samples with dimensions of 150 × 150 × 150 mm. Compressive strength tests were carried out with a Yuksel Kaya brand press device with a

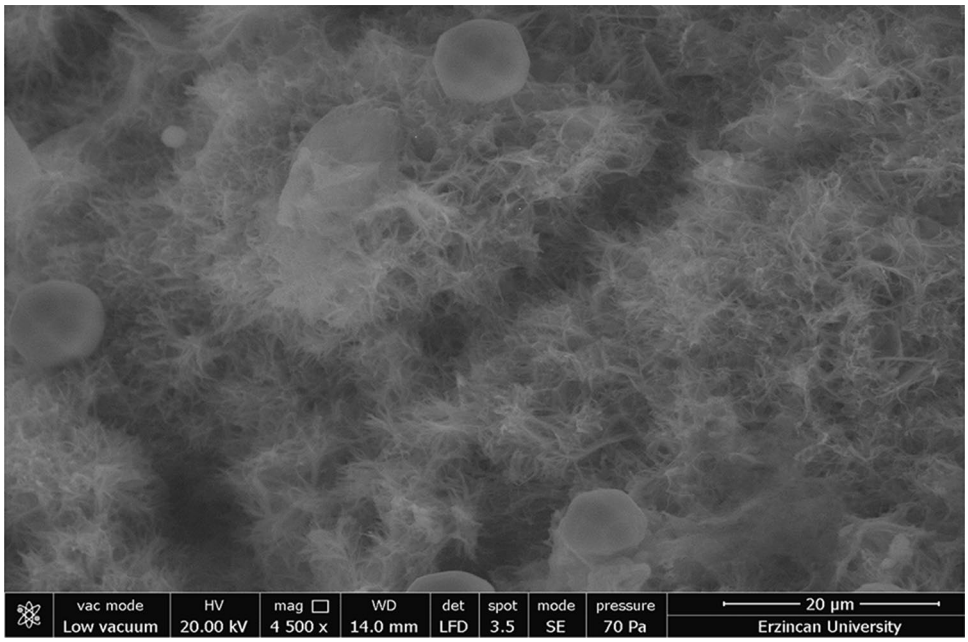

Fig. 2 Structure of the natural perlite; SEM magnification × 4.500

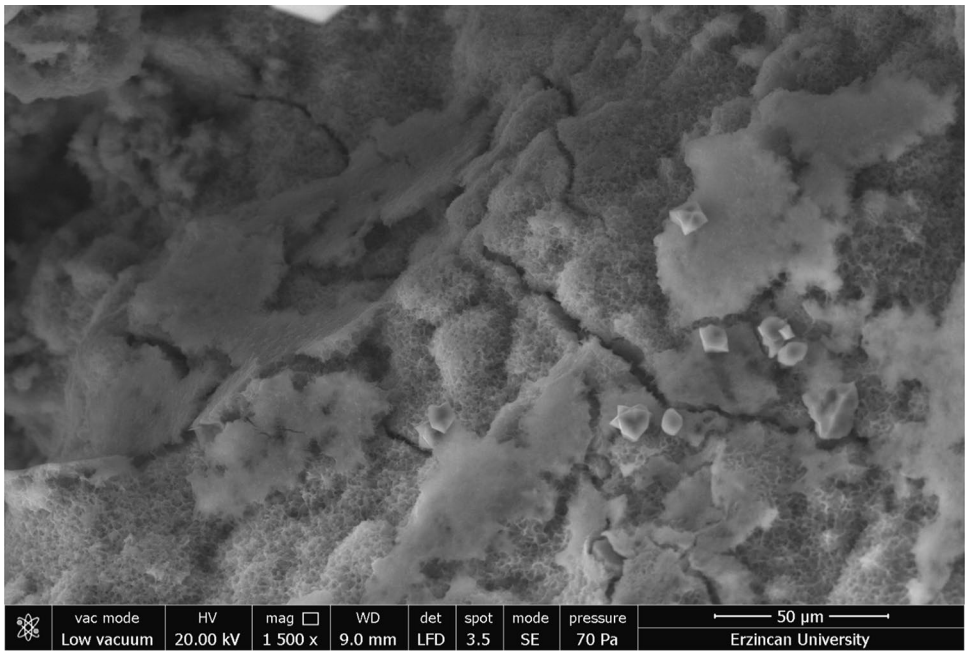

Fig. 3 Structure of the natural perlite; SEM magnification × 1.500

Table 4 Conformance of the natural perlite aggregates to ASTM C 618

	Natural perlite Aggregates	ASTM C 618
$SiO_2 + Al_2O_3 + Fe_2O_3$ (%)	87.10	Min. 70.0
SO_3 (%)	0.05	Max. 4.0
Loss on ignition (%)	3.27	Max. 10.0
Fineness: amount retained when wet-sieved on 45 µm sieve (%)	30	Max. 34.0
Strength index 7-days (%)	78	Min. 75.0
Strength index 28-days (%)	80	Min. 75.0

capacity of 3000 kN. The loading rate in compression tests was selected as 0.4 MPa/s. The visual of the compressive strength test is given in Fig. 4. Ultrasonic pulse velocity (UPV) test was carried out on 150 × 150 × 150 mm cube specimens of 28, 56, and 90 days old. A transmitter and receiver probe were installed on parallel surfaces of the specimen, and the time interval of the sound was recorded. The ultrasonic gel used in the UPV test provides a medium to ensure continuous sound transmission on the surface where the probe contacts the concrete. Then, the velocity of sound in concrete is calculated by Eq. (1) (Marie 2016).

Table 5 Concrete mix design (kg/m^3)

Code	Cement	Natural Perlite	Fine Agg	Coarse Agg	Water	Superplasticizer (%)
C	450.00		834.36	840.63	202.5	0.7
NP10	450.00	126.41	750.92	756.57	202.5	0.7
NP20	450.00	252.82	667.49	672.51	202.5	0.7
NP30	450.00	379.23	584.05	588.44	202.5	0.7
NP40	450.00	505.64	500.62	504.38	202.5	0.7
NP50	450.00	632.04	417.18	420.32	202.5	0.7
NP75	450.00	948.07	208.59	210.16	202.5	0.7
NP100	450.00	1264.09			202.5	0.7

Fig. 4 Images of compressive strength

$$V = L/t \tag{1}$$

L in Eq. (1) represents the distance traveled by the sound between the two probes (0.15 m), and *t* represents the experimentally measured sound transmission time in seconds. Finally, *V* is the speed of sound in m/s.

Once the ultrasonic pulse velocity measurements were acquired for the concrete samples, and the average velocities were determined for each specimen, the dynamic modulus of elasticity was calculated using the methodology outlined in ASTM C 597 (2016). Specifically, Eq. (2) from the ASTM standard (ASTM 2016) was utilized to compute the dynamic modulus of elasticity.

$$E_d = \frac{\rho V^2(1+\mu)(1-2\mu)}{1-\mu} \tag{2}$$

In Eq. (2), E_d represents the dynamic modulus of elasticity of concrete (MPa), and ρ demonstrates the density of concrete (kg/m^3). At the same time, *V* is the ultrasonic pulse velocity (km/s), and μ is the Poisson's ratio of the concrete.

The capillary absorption test of concrete specimens was carried out according to the ASTM C 1585 (2020) standard. The specimens were dried in an oven at a temperature of 70 ± 7 °C for 24 h to constant weight, then cooled at ambient temperature and dry weighed (W_0). The dimensions of the surface area (F, cm^2) of the specimens in contact with water were measured with a caliper. Afterward, the samples were placed in a container of water, and the amount of water absorption of each sample at 1–4–9–16–16–25–36–49–49–64–81 min (t, min) was weighed on a precision balance, and mass increments were measured (Q, cm^3). With the data obtained, the amount of water absorbed from the unit area of each sample was calculated, and a curve was sketched with the square root of the time elapsed during the experiment ($\sqrt{t}$) on the horizontal axis and the amount of water absorbed per unit area on the vertical axis. Capillary water absorption coefficient values were calculated with the slope of this curve. These values obtained from the curve were also evaluated with Eq. (3).

$$K = \frac{Q}{F.\sqrt{t}} \tag{3}$$

In Eq. (3), K stands for the capillary absorption coefficient, Q for the amount of water absorbed, F for the base area of the specimens in contact with water, and t for the time

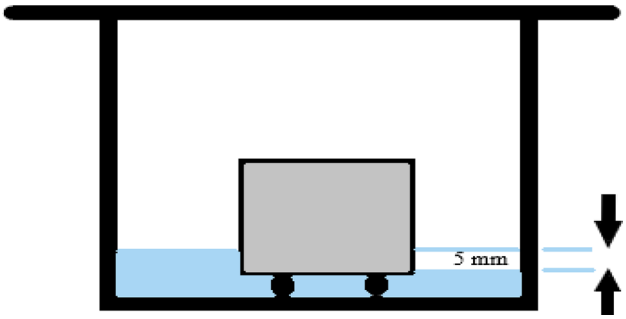

Fig. 5 The schematic test setup for the capillary water absorption test

the specimens were in contact with water. Capillary water absorption tests were performed on 28, 56, and 90 days aged cube specimens. The schematic test setup showing the capillary water absorption test is given in Fig. 5.

In order to make measurements independent of the effect of moisture conditions, the electrical resistance value (R) was measured with a resistance meter (ohmmeter) according to the two-plate method in accordance with ASTM C 1760 (2012) standard on oven-dried concretes. Three repeated measurements were performed from each series and arithmetic mean values were calculated. The electrical resistivity values of the concrete, for which resistance values (*R*) were measured, are determined using Eq. (4).

$$\delta = R\frac{A}{L} \tag{4}$$

In the equation, δ represents electrical resistivity (kohm.m); *R* represents resistance (kohm); A represents sample surface area (m^2); and *L* represents the distance between plates (m). The electrical resistivity test was conducted on 28, 56, and 90 days aged cube specimens. The visual representation of the electrical resistivity test apparatus is given in Fig. 6.

To assess the response of concrete specimens to aggressive environmental conditions, acid, and sulfate attack tests were performed on cube specimens in accordance with the ASTM C 267 (2020) and ASTM C 1012 (2019) standards, respectively. Two specimens of each concrete were exposed to 5% H_2SO_4 and 5% Na_2SO_4 solutions for 28, 56, and 90 days. The prepared solutions were replaced every four weeks. The concretes were removed from the solutions, washed with clean tap water to remove loose reaction products, dried with a towel, and then allowed to dry at room temperature before weighing and visual inspection. The visual evaluation was also carried out to critically observe the physical durability effect of the specimens in H_2SO_4 and Na_2SO_4 solutions.

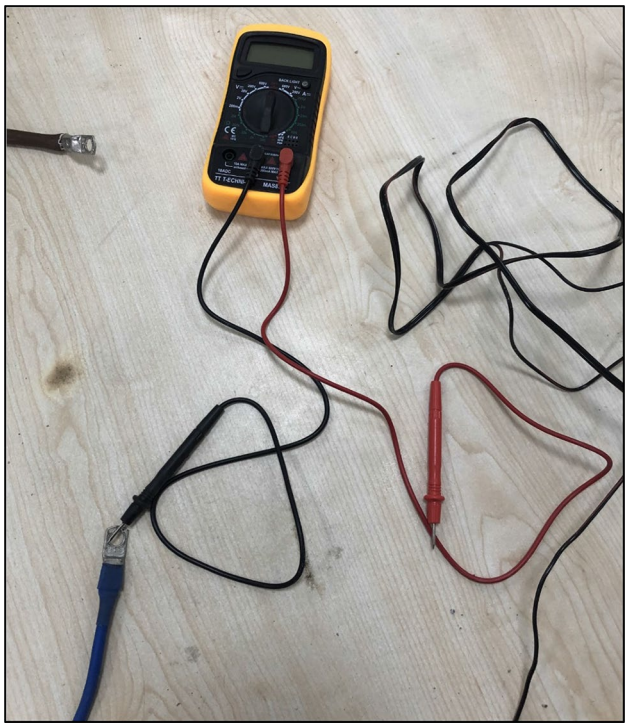

Fig. 6 The visual representation of the electrical resistivity test apparatus

The evaluation was based on the condition of the specimens' edges, surface texture, color, size, and shape. After the visual assessment, the specimens were weighed for weight loss; hence, the percentage weight loss, and pre- and post-exposure compressive strengths were calculated. The concrete visuals after being exposed to acid and sulfate tests are given in Fig. 7.

3 Results and discussion

3.1 Fresh density

The fresh density test results of the concrete are presented in Fig. 8. As can be noticed in Fig. 8, with the use of natural perlite in the mixtures at increasing rates, the fresh density results decreased compared to the control concrete. The fresh densities of the concretes varied between 2353 and 1944 kg/m^3 depending on the perlite contents. While the control concrete had the highest fresh density value with 2353 kg/m^3, the sample coded NP100 had the lowest fresh density value with 1944 kg/m^3.

When 100% natural perlite was used in the mixtures, weight losses of 17.38% per fresh density occurred compared to the control concrete. The primary cause of this reduction is attributed to the disparity in specific gravity between natural perlite (2.015 g/cm^3), which replaces

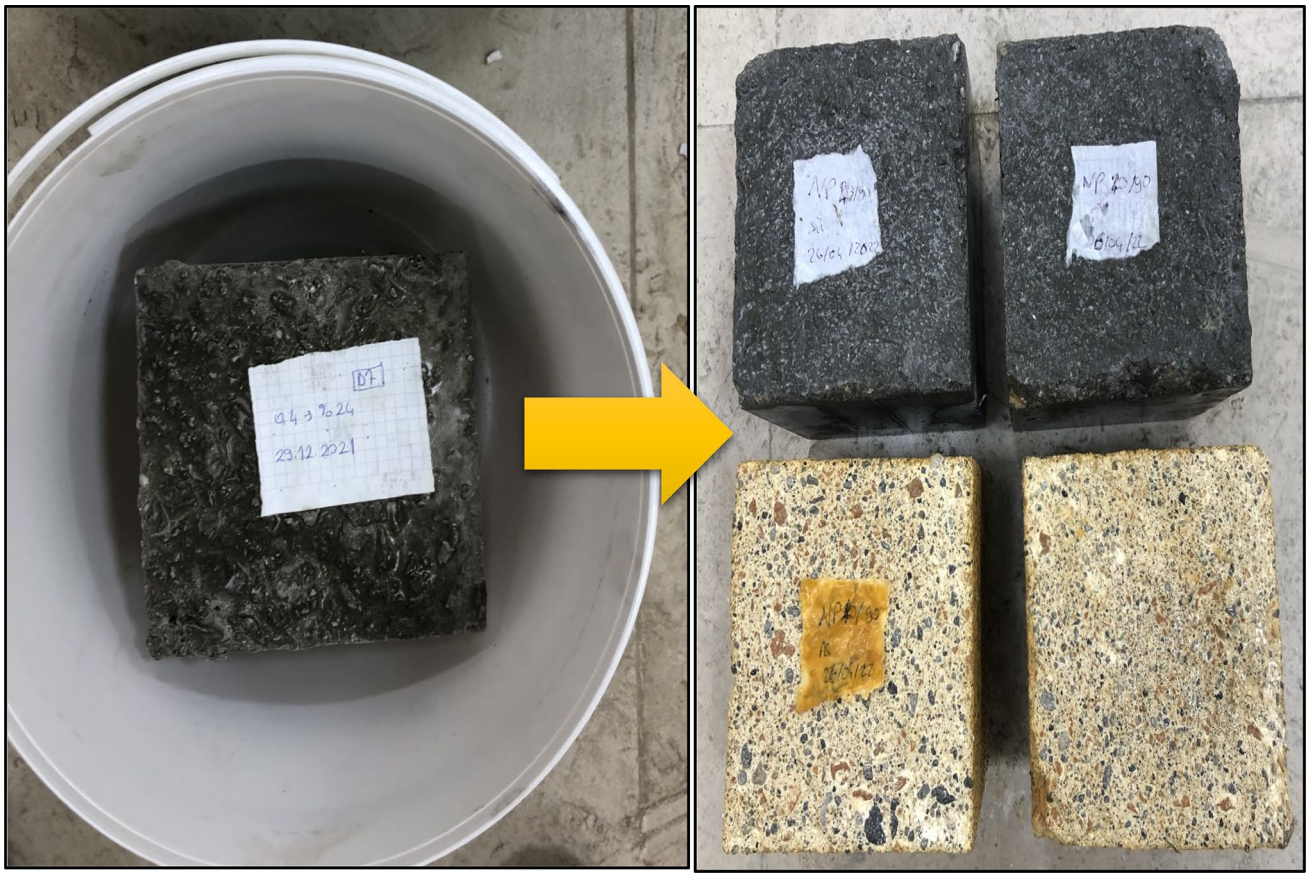

Fig. 7 Images of concretes after being exposed to acid and sulfate tests

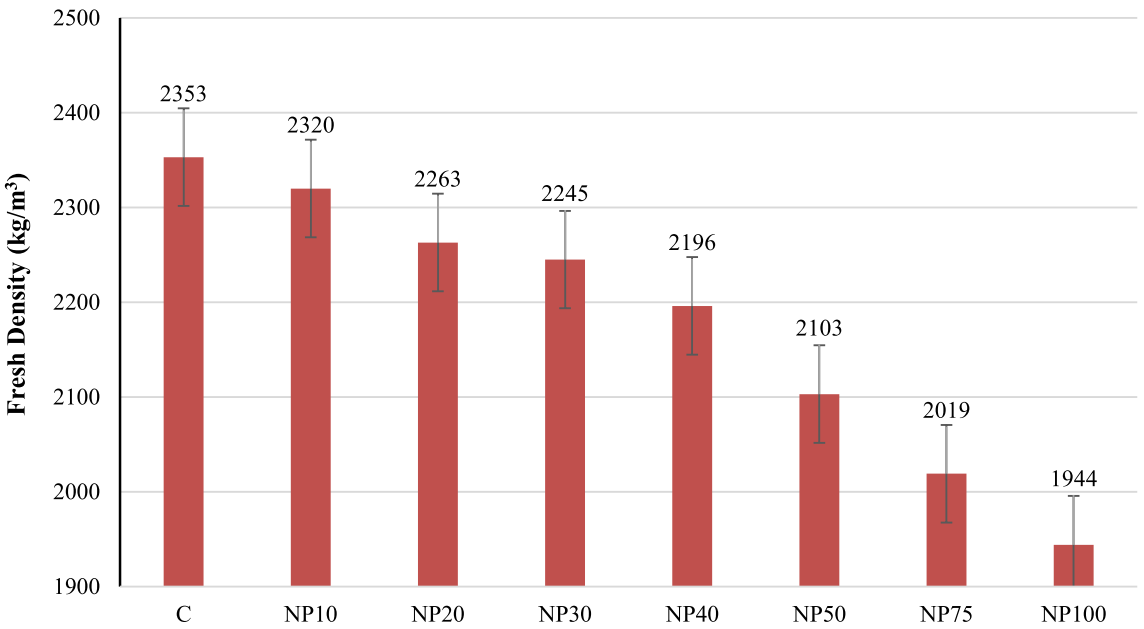

Fig. 8 Relationship between fresh densities of the mixes

Table 6 Compressive strength test results

Code	Compressive Strength (MPa)
C/28	51.7
C/56	56.1
C/90	60.8
NP10/28	51.1
NP10/56	57.1
NP10/90	62.4
NP20/28	46.8
NP20/56	54.2
NP20/90	55.4
NP30/28	43.5
NP30/56	47.6
NP30/90	49.7
NP40/28	35.2
NP40/56	39.4
NP40/90	43.8
NP50/28	34.2
NP50/56	38.2
NP50/90	42.5
NP75/28	31.9
NP75/56	37.8
NP75/90	40.4
NP100/28	28.7
NP100/56	35.4
NP100/90	39.5

crushed stone and natural river sand, and the latter materials with specific gravities of 2.68 g/cm^3 and 2.66 g/cm^3, respectively. The lower specific gravity of natural perlite leads to a decrease in the overall density of the concrete mixture. Similar results were obtained in the studies conducted in Refs. (Pasupathy et al. 2022; Ragul et al. 2022; Wang et al. 2022). As can be observed as a result of this study, the low fresh density values of lightweight concretes produced utilizing natural perlite aggregate can reduce the weight of the structural elements and thus provide concretes with higher earthquake resistance (Sengul et al. 2011).

3.2 Compressive strength

Table 6 and Fig. 9 display the compressive strength test results. Accordingly, the lowest compressive strength was obtained from sample NP100/28 with 28.70 MPa, and the highest compressive strength was obtained from sample NP10/90 with 62.42 MPa with 117% increase. Using 10% natural perlite in the mix, the compressive strength of the concretes increased on all the measured days. The 28-day compressive strength of concrete with 10% natural perlite (NP10/28), which was slightly lower than the control concrete (C/28), exceeded the control concrete at advanced ages (56 and 90 days). As the perlite content increased, the compressive strengths decreased compared to the control concrete. Similar findings were obtained in the studies conducted in Refs. (Topçu and Işıkdağ 2008; Sengul et al. 2011; Sayadi et al. 2018; Akyuncu and Sanliturk 2021; Ragul

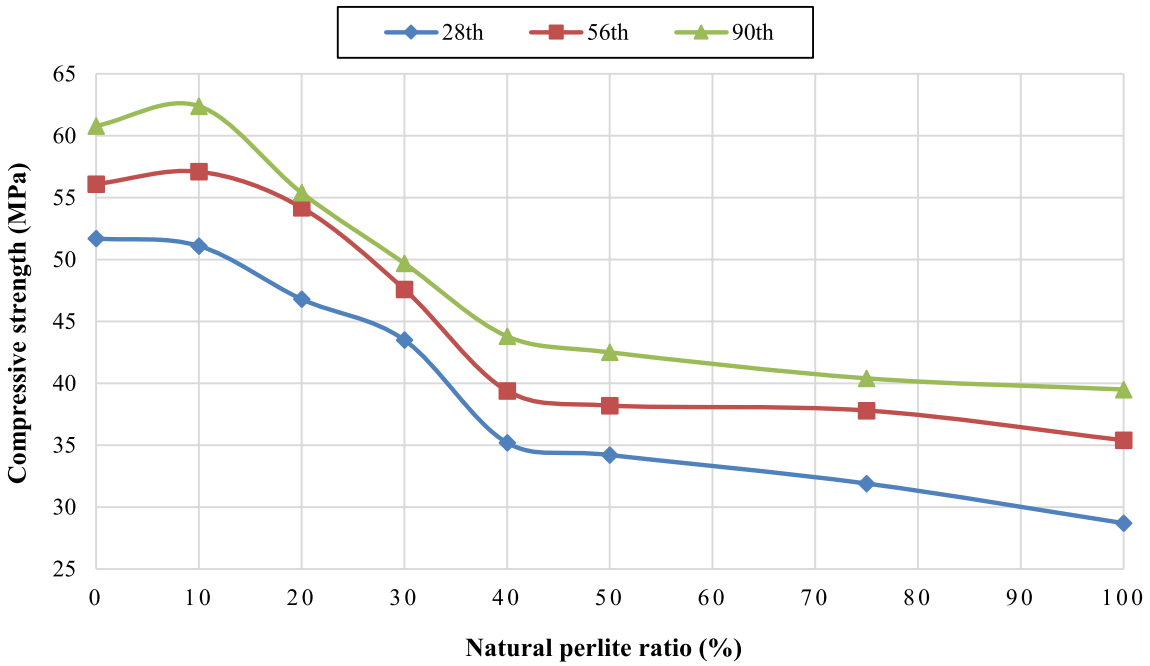

Fig. 9 Relationship between compressive strength and replacement rate of natural perlite

et al. 2022). It was stated that the decrease in compressive strength was due to less integrity between the cement paste and perlite aggregate (Top et al. 2020). In addition, it has been reported that the properties of perlite, such as its lower specific gravity, hollow structure, and increased need for mixing water, have a negative effect on compressive strength results (Oktay et al. 2015; Różycka and Pichór 2016). The negative effect of the increased utilization of natural perlite on the compressive strength may have originated from the porous structure of perlite. The increase in porosity resulted in loss of density and strength (Rashad 2016).

While the 90-day compressive strength of the control concrete (C/90) was 60.8 MPa, the 90-day compressive strength of concrete produced from 100% natural perlite (NP100/90) decreased by 35% to 39.5 MPa. For all groups, concrete compressive strengths increased as the number of days increased. When the curing period increased from 28 to 90 days, the compressive strength increases in the concretes were approximately 14–37%. It is believed that perlite's pozzolanic property effectively increases strength at advanced ages. Some researchers (Ramezanianpour et al. 2014; Mir and Nehme 2017; Karein et al. 2018; Esfandiari and Loghmani 2019; Junaid et al. 2022) have also reached similar findings. It was also observed during the concrete production phase that 10% of natural perlite aggregate had a superior adherence with cement and other components, resulting in a concrete with ideal workability. This is estimated to have a favorable effect on the compressive strength. When natural perlite is present in proportions higher than 10%, compressive strength losses are believed to occur as a result of the increase in the volume and size of the pores both in the cement paste and in the interfacial transition zone (ITZ). Similar observations have been reported in other studies (Kotwica et al. 2017; Karein et al. 2018). This study proved that the optimum compressive strength can be achieved using 10% of natural perlite in concrete. It was also proved that lightweight concretes with high strength of 50 MPa and above can be produced by using 10% (for all days) and 20% (after 56 days) perlite.

3.3 Ultrasonic pulse velocity

Table 7 and Fig. 10 demonstrate the results of the ultrasonic pulse velocity test (UPV). According to Fig. 10, UPV values decreased for all days due to increased natural perlite content in the concrete. When the 28-day UPV results are evaluated among themselves, it is observed that the highest UPV was obtained from the control concrete (C/28) with 5093 m/s and the lowest UPV was obtained from the concrete with 100% natural perlite (NP100/28) with 4300 m/s. The reduction in UPV value between these two concretes was approximately 16%. The UPV values decreased sharply, especially after using 50% natural perlite in the concrete.

Table 7 UPV test results

Code	UPV (m/s)
C/28	5093
C/56	5276
C/90	5439
NP10/28	5037
NP10/56	5200
NP10/90	5291
NP20/28	4946
NP20/56	5120
NP20/90	5102
NP30/28	4926
NP30/56	5045
NP30/90	5034
NP40/28	4835
NP40/56	4954
NP40/90	5005
NP50/28	4780
NP50/56	4847
NP50/90	4992
NP75/28	4386
NP75/56	4405
NP75/90	4651
NP100/28	4300
NP100/56	4192
NP100/90	4467

For instance, when the 56-day results are analyzed, the UPV value of 75% natural perlite concrete (NP75/56) is 8% lower than that of 50% natural perlite concrete (NP 50/56). On the other hand, when the 28-day results were analyzed, the UPV difference between 100% natural perlite concrete (NP 100/28) and 50% natural perlite concrete (NP 50/28) was 14%. Similar results were observed for 56 and 90 days old concretes. It was noticed that the UPVs increased with the increase in curing time from 28 to 90 days. This phenomenon can be explained by the pozzolanic property of perlite, which improves the hydration of binder materials and fills cracks and voids in the cement paste (Mir and Nehme 2017). The study revealed that the increase in UPV of 90-day specimens can reach up to 7% compared to 28-day specimens, regardless of the proportion of natural perlite. UPV experiments can be useful to investigate the relationship between permeability and the void structure of concrete (van Jaarsveld and van Deventer 1999). This phenomenon can be attributed to the porous and hollow structure of perlite, which affects the propagation of ultrasonic waves through the material, resulting in a decrease in UPVs (Othman et al. 2020; Akyuncu and Sanliturk 2021; Polat 2022). Since it is recognized that ultrasonic waves move more slowly in hollow environments, it can be stated that obtaining a more porous structure with the substitution of natural perlite in

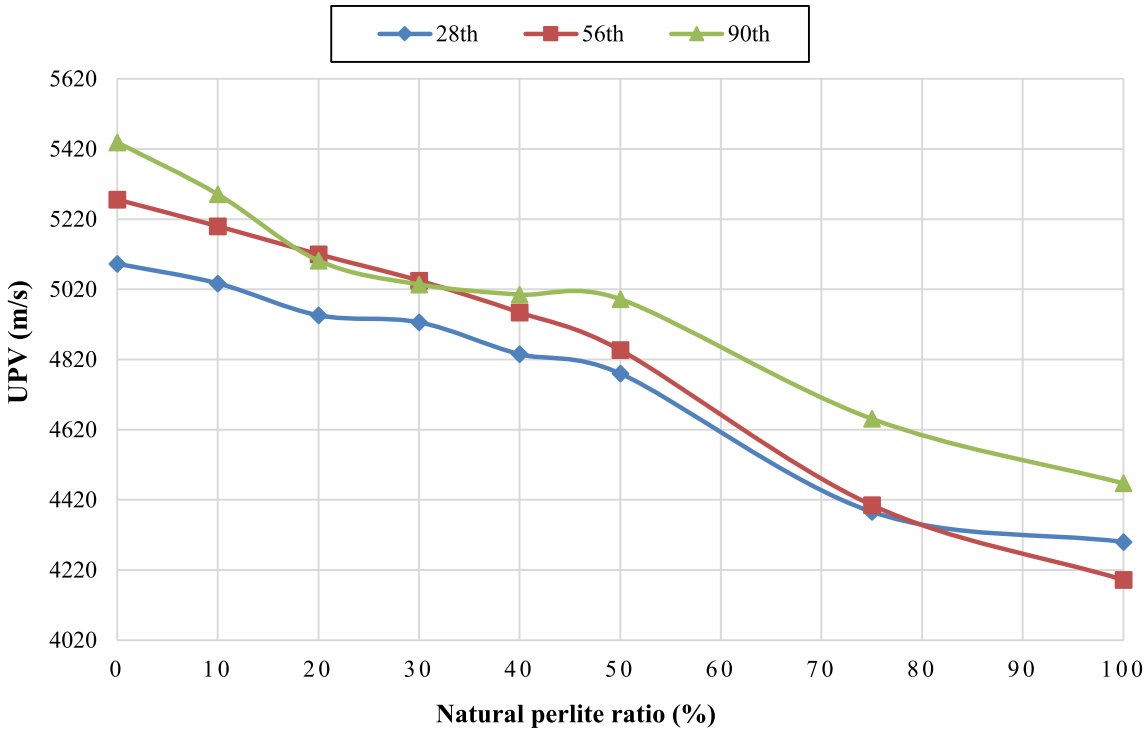

Fig. 10 Relationship between UPV values and natural perlite ratio

the concrete internal structure is effective in the decrease of UPV values (Huang et al. 2021; Karakaş et al. 2023). In addition, as a result of this study, UPVs of concretes with natural perlite generally exhibited similar behavior to the compressive strength (Chinnu et al. 2021). The IS 13311 (1992) standard classifies concretes with UPVs greater than 4500 m/s as excellent quality concrete. In addition, concretes with UPV values of 3500–4500 m/s are also classified as quality concrete. According to this standard, concretes containing 75–100% perlite were classified as good quality, while all others were classified as excellent. As a result of this study, it has been proved that good or excellent concrete can be produced with concrete produced using perlite in terms of the UPV test.

3.4 Dynamic modulus of elasticity

The dynamic modulus of elasticity results are presented in Table 8 and Fig. 11.

In order to determine the dynamic modulus of elasticity, the density and UPV values obtained from the concretes were utilized along with Eq. (2). Also, Poisson's ratio was regarded as 0.2 (Rao et al. 2016; Thomaz et al. 2021). Accordingly, it was observed that the dynamic modulus of elasticity of the concretes decreased with the increase in the proportion of natural perlite. When the 90-day dynamic modulus of elasticity results was evaluated, it

Table 8 Dynamic modulus of elasticity test results

Code	Dynamic modulus of elasticity (GPa)
C/28	54.9
C/56	59
C/90	62.7
NP10/28	53
NP10/56	56.5
NP10/90	58.4
NP20/28	49.9
NP20/56	53.4
NP20/90	53
NP30/28	49.1
NP30/56	51.5
NP30/90	51.1
NP40/28	46.3
NP40/56	48.4
NP40/90	49.4
NP50/28	43.2
NP50/56	44.5
NP50/90	47.1
NP75/28	35
NP75/56	35.3
NP75/90	39.6
NP100/28	32.4
NP100/56	30.7
NP100/90	35

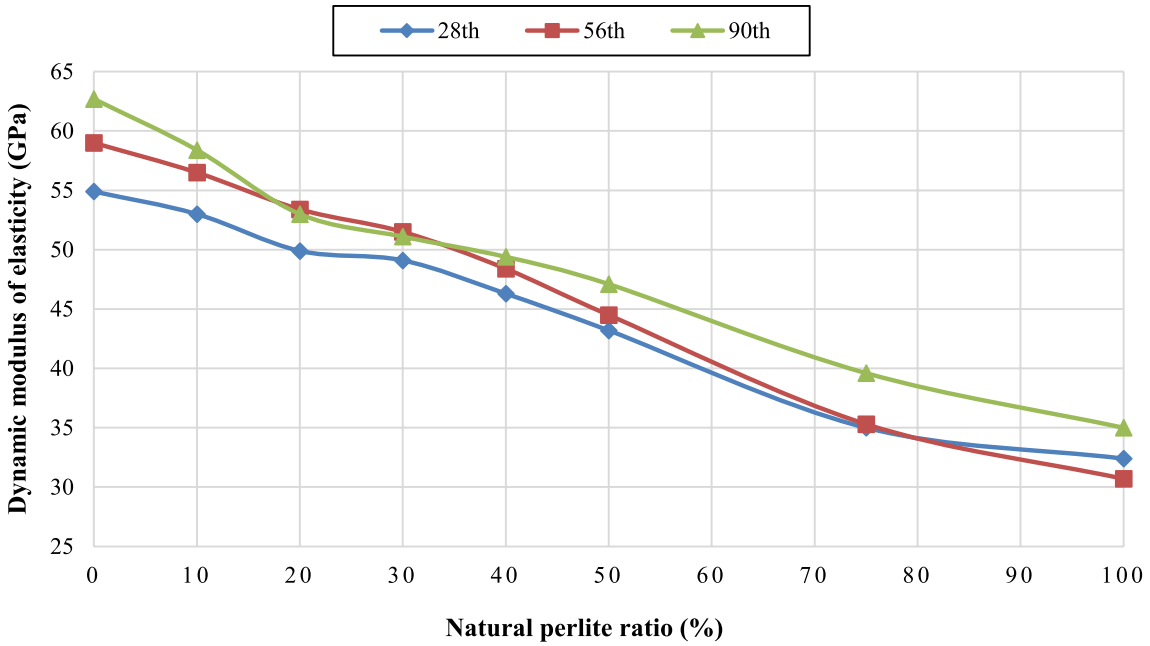

Fig. 11 Relationship between dynamic modulus of elasticity and replacement ratio of natural perlite

was determined that the highest dynamic modulus of elasticity was obtained from the control concrete (C/90) with 62.7 GPa, and the lowest was obtained from the concrete produced from 100% natural perlite coded NP100/90 with 35 GPa. The reduction in the dynamic modulus of elasticity between these two concretes was approximately 45%. As with the UPV results, the dynamic modulus of elasticity values decreased significantly after using 50% perlite in the concrete. Similar behavior was observed for 28- and 56-day-old concretes. The decrease in the dynamic modulus of elasticity values is in line with the findings in the literature (Topçu and Uygunoğlu 2010; Sengul et al. 2011; Ashtiani et al. 2014; Li et al. 2021). This is believed to be because the replacement of natural perlite with crushed stone at increasing ratios resulted in concretes with lower compressive strengths, resulting in decreases in the dynamic modulus of elasticity values (Topçu and Uygunoğlu 2010; Sayadi et al. 2018). As a result of extending the curing period from 28 to 90 days, the dynamic modulus of elasticity values of the concretes increased. The experimental results indicated that the increase in the dynamic modulus of elasticity of concretes cured for 90 days can be up to 14% compared to concretes cured for 28 days.

3.5 Capillary absorption

Table 9 and Fig. 12 present the coefficients obtained due to the capillary absorption test of the concretes. As can be seen from Fig. 12, the capillary absorption coefficients for all

Table 9 Capillary absorption test results

Code	Capillary absorption coefficient ($\times 10^{-5}$ g/cm^2 sn^{0,5})
C/28	26
C/56	23
C/90	18
NP10/28	28.81
NP10/56	27.98
NP10/90	19
NP20/28	30.45
NP20/56	28.75
NP20/90	21.23
NP30/28	32.92
NP30/56	29.38
NP30/90	24.69
NP40/28	34.61
NP40/56	31.75
NP40/90	28.22
NP50/28	37.24
NP50/56	33.19
NP50/90	30.16
NP75/28	40.23
NP75/56	36.56
NP75/90	32.49
NP100/28	43.43
NP100/56	39.14
NP100/90	35.01

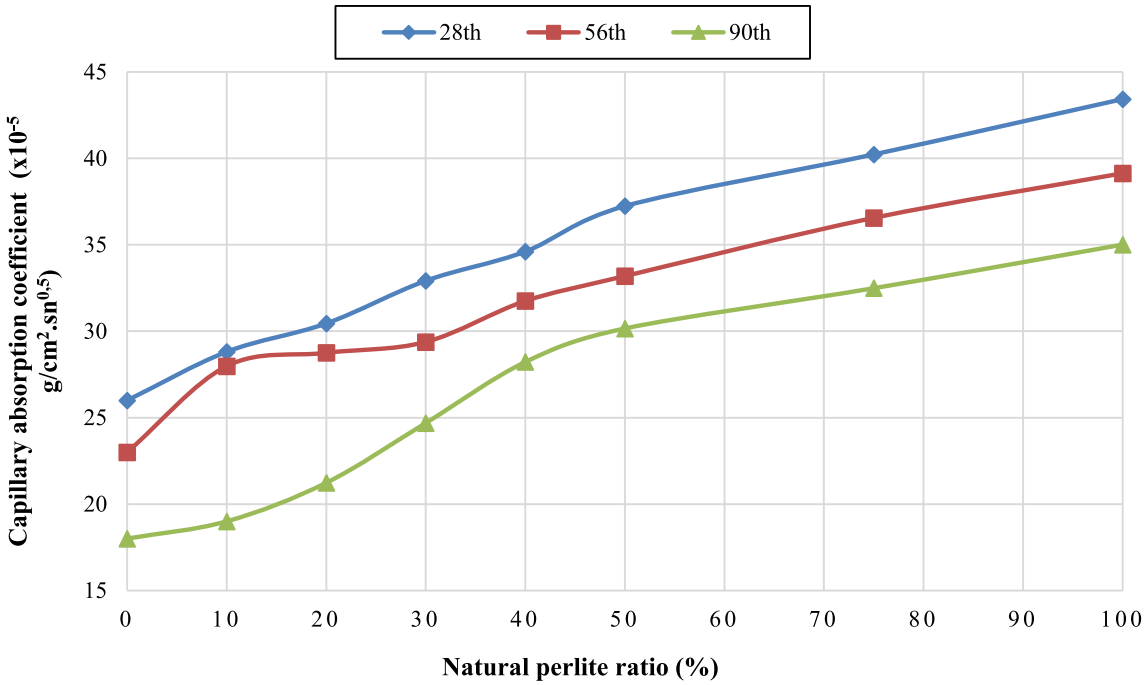

Fig. 12 Relationship between capillary absorption and replacement rate of natural perlite

days increased as the natural perlite utilization rate increased in the mixtures.

Among all groups, the highest capillary absorption coefficient was 43.43 in concrete produced from 100% natural perlite (NP100/28), and the lowest capillary absorption coefficient was 18 in control concrete (C/28). Capillary absorption coefficient increases of up to 67% were realized due to the use of natural perlite in the concretes compared to the control concrete. This is attributed to the fact that the replacement of high water absorption perlite aggregate with natural aggregate leads to the formation of a more porous microstructure in the matrix, and the concrete series with increased perlite content continuously increases the capillary absorption coefficient (Sengul et al. 2011; Esfandiari and Loghmani 2019; Akyuncu and Sanliturk 2021; Chinnu et al. 2021). Concretes produced with natural perlite exhibited high levels of sorptivity due to the natural water absorption capacity of the material (Torres and García-Ruiz 2009). As the curing time increased, the capillary absorption coefficients of all groups decreased. Other studies also observed a similar pattern (Mir and Nehme 2017; Gencel et al. 2022). It has been reported that capillary absorption values can be reduced in the long term due to the development of perlite-induced pozzolanic reactions which also increase compressive strength over time (Guenanou et al. 2019).

Table 10 Electrical resistivity test results

Code	Electrical resistivity (kΩ-m)
C/28	54.73
C/56	55.97
C/90	58.14
NP10/28	52.71
NP10/56	55.73
NP10/90	60.65
NP20/28	42.86
NP20/56	53.41
NP20/90	59.92
NP30/28	41.38
NP30/56	56.06
NP30/90	61.43
NP40/28	60.81
NP40/56	76.27
NP40/90	78.74
NP50/28	57.14
NP50/56	87.93
NP50/90	90
NP75/28	52.68
NP75/56	105.57
NP75/90	117.65
NP100/28	52.48
NP100/56	95.74
NP100/90	139.75

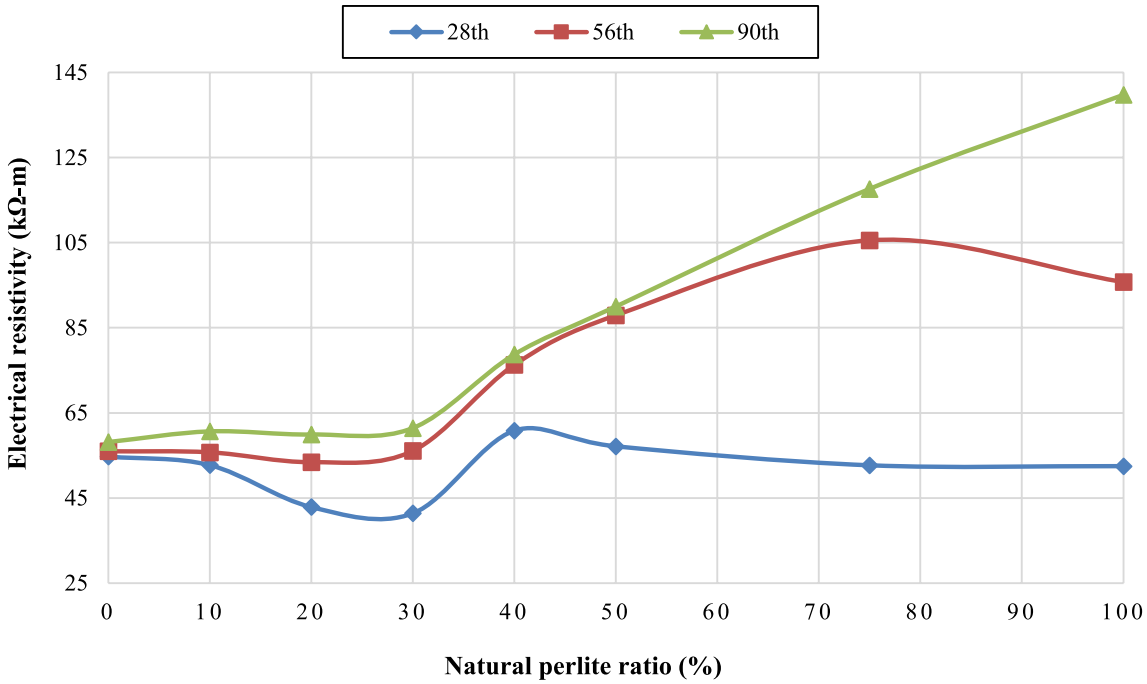

Fig. 13 Relationship between electrical resistivity of the mixes

3.6 Electrical resistivity

The electrical resistivity values of the concrete are presented in Table 10 and Fig. 13. According to Fig. 13, it is visible that the use rate of natural perlite is very effective on the electrical resistivity results. Especially when 40% natural perlite was used in concrete production, electrical resistivity values increased dramatically for all days.

For example, while the electrical resistivity value of the control concrete for 56 days (C/56) was 55.97 kΩ-m, this value increased by 36% to 76.27 kΩ-m after the use of 40% natural perlite in the concrete (NP40/56). This situation was observed similarly in the 90-day results. At advanced ages (56 and 90 days), the concretes' electrical resistivity increased with the use of natural perlite. Similar results were also observed in studies in the literature (Ramezanianpour et al. 2014; Karein et al. 2018). Among all groups, the concrete with the highest electrical resistivity at 56 days was produced from 75% natural perlite with a value of 105.57 kΩ-m (NP75/56). The electrical resistivity value increased by 100% compared to 28 days and 89% compared to the control concrete. At the end of 90 days, the highest electrical resistivity value among the concretes was obtained in the mixture produced from 100% natural perlite (NP100/90) with a value of 139.75 kΩ-m. This value is the highest electrical resistivity value among all groups, and it is 166% higher than 28 days and 140% higher than the control concrete. The electrical resistivity of concrete represents the potential to retain the movement of charged ions through the concrete matrix, meaning that it exhibits an inversely proportional relationship with the corrosion risk of concrete, with a higher electrical resistivity representing a lower risk of corrosion formation (Sayadi et al. 2018; Adhikary et al. 2022). This study proved that corrosion risk can be reduced by producing concretes with high electrical resistivity due to the use of natural perlite. In addition, this study also proved that concrete with high electrical resistivity, or insulating concretes, can be obtained by using increasing amounts of natural perlite in the concrete.

3.7 Acid attack

The acid-attacked concrete was visually evaluated, along with the specimens' weight loss and compressive strength.

3.7.1 Weight loss of acid attacked concretes

The graphic representing the weight loss (%) of the concretes subjected to acid attack for 28, 56, and 90 days is given in Fig. 14.

Accordingly, the weight loss percentages of the concrete subjected to acid attack for 28 days decreased with the increase in natural perlite utilization. Compared to the control concrete (C/28), the weight loss of concrete produced from 100% natural perlite (NP100/28) was 85% less. When the 56-day results were analyzed, although the weight loss values for all groups were very close, the weight loss increased, especially up to 50% natural perlite utilization

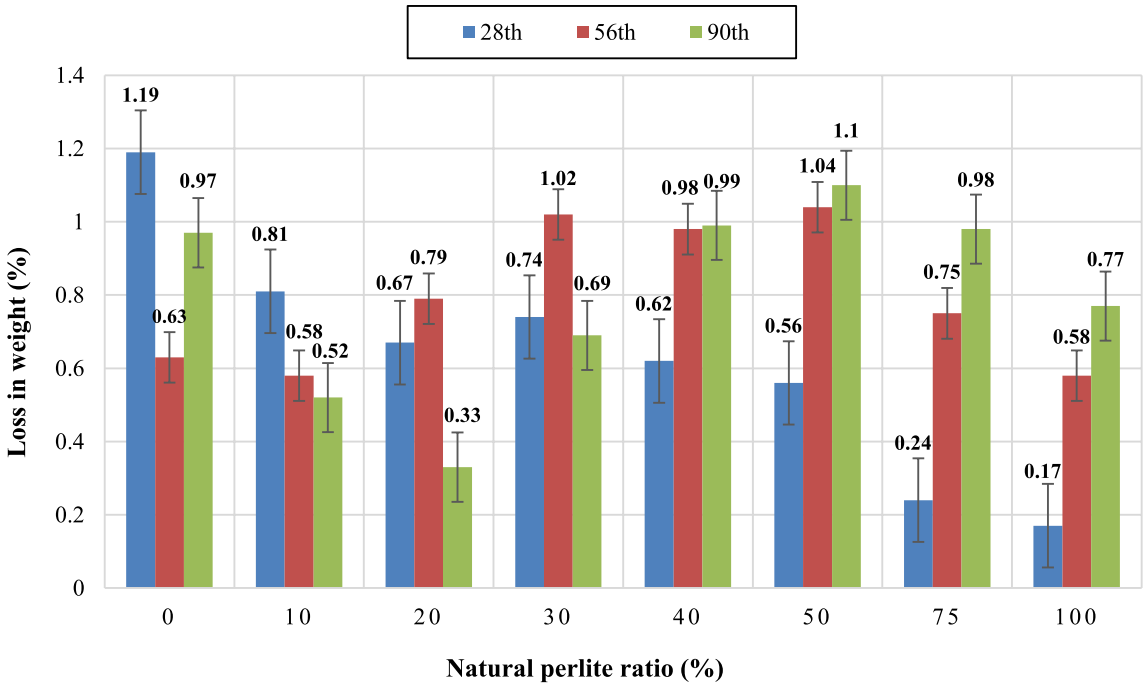

Fig. 14 Loss in weight of acid attacked concretes

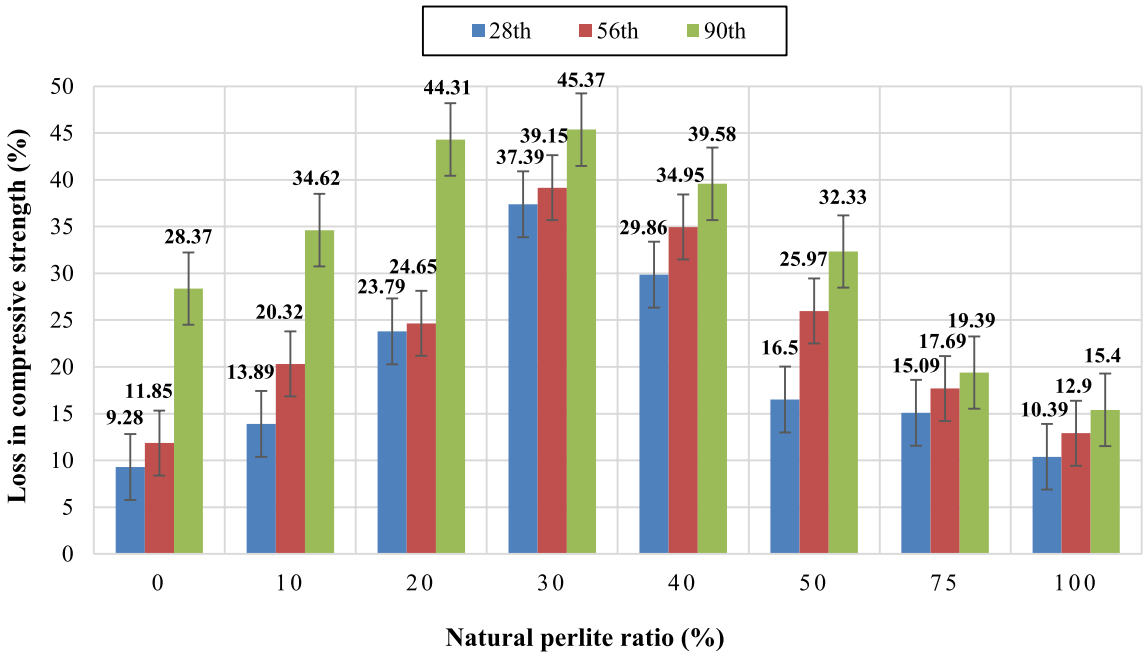

Fig. 15 Loss in compressive strength of acid attacked concretes

rate, and decreased again after this. Similar behavior was observed in the 90 day results. The most important aspect to be deduced from the weight loss results is that the acid resistance of the concrete produced using natural perlite is significantly higher. This result was clearly obtained when compared with the control concrete. Compared to the control concrete, the weight loss of concrete produced with 100% natural perlite was 86%, 8% and 21% less after 28, 56 and 90 days of acid attack, respectively.

3.7.2 Compressive strength loss of acid attacked concretes

Figure 15 illustrates the percentage loss in compressive strength of concrete exposed to the acid solutions for 28, 56, and 90 days.

It can be noted from Fig. 15 that the compressive strength losses of the acid-attacked concretes were highest for all days when 30% natural perlite was used and then showed a decreasing pattern. For example, when the results of 56 days are evaluated, it is observed that the compressive strength loss of the control concrete (C/56) is 11.85%, 39.15% for concrete with 30% natural perlite (NP30/56), and 12.9% for concrete with 100% natural perlite (NP100/56). Losses in compressive strength increased dramatically in the concretes with 30% natural perlite and then began to decrease. The strength losses in the concrete with 100% natural perlite and the control concretes were almost equal. Although the 90-day results were similar, the losses in the compressive strength of the concrete produced using high percentages (75% and 100%) of natural perlite were less than those of the control concrete. This study determined that the perlite utilization rate greatly affects the losses in compressive strength due to acid attack. 30% was determined to be the critical rate, especially for the concretes produced using 75% and 100% natural perlite, which exhibited high resistance to acid attack.

Finally, the visual results of the specimens after the acid attack were evaluated through Figs. 16 and 17. Figure 16 clearly illustrates a correlation between weight and compressive loss results and the condition of concrete surfaces. The control concrete and those composed of 100% natural perlite exhibited lesser damage and displayed higher resistance to acid exposure. In contrast, the concrete containing 30% natural perlite showed significant exfoliation on the top layer due to the influence of sulfuric acid, rendering it the least resistant among the tested specimens.

In Fig. 17, it is confirmed by the visual results that as the acid exposure period progresses (from 28 to 90 days), the deterioration of the concrete is more significant. However, the least in control and 100% natural perlite concrete and the most in concrete with 30% natural perlite..

3.8 Sulfate attack

A comprehensive visual assessment of the sulfate affected concretes was conducted in conjunction with the examination of weight loss and compressive strength data obtained from the specimens.

3.8.1 Weight loss of sulfate attacked concretes

The graphic indicating the weight loss (%) of the concretes subjected to sulfate attack for 28, 56, and 90 days is provided in Fig. 18. Figure 18 shows that the weight losses of the concretes were very similar for all days due to the sulfate attack. For instance, the percentage weight loss of concrete exposed to sulfate attack for 28 days ranged from 0.95 to 1.17, whereas at 90 days the range was 1.1 to 1.33. The difference between the weight loss of control concrete and concrete produced from 100% natural perlite after sulfate attack as a function of age ranged from 2 to 19%. A similar pattern was observed for 56 days. Even if the proportion of

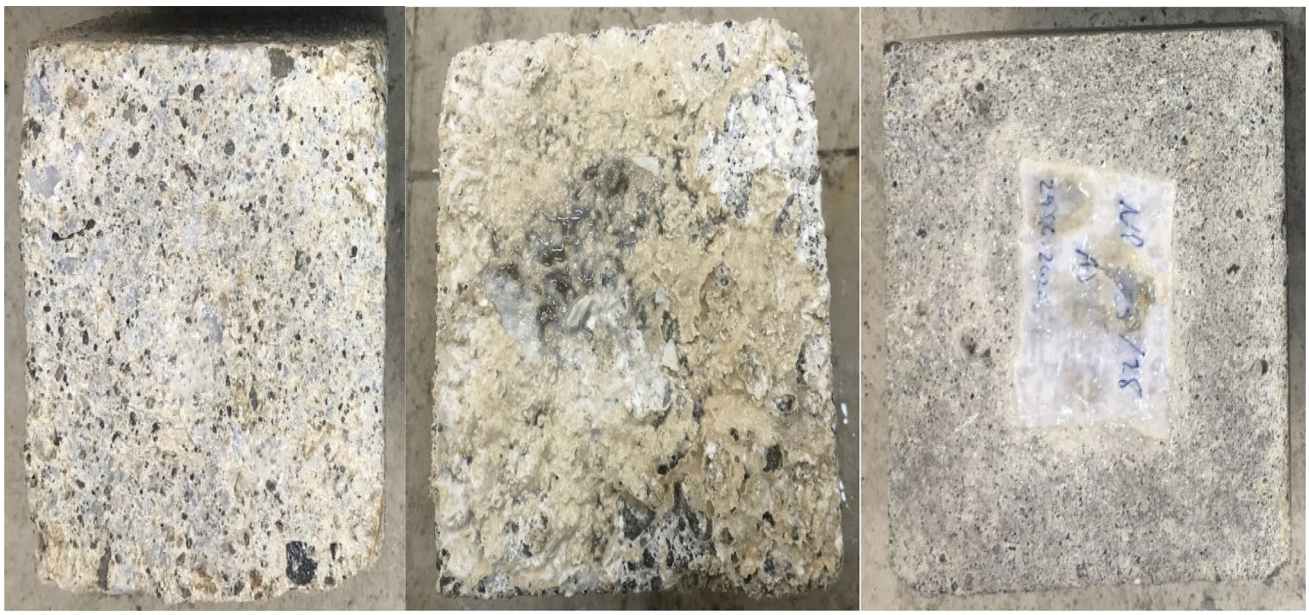

Fig. 16 Images of concrete exposed to acid attack for 28 days. Concretes containing 0%, 30% and 100% natural perlite

Fig. 17 Images of concrete exposed to acid attack for 90 days. Concretes containing 0%, 30% and 100% natural perlite

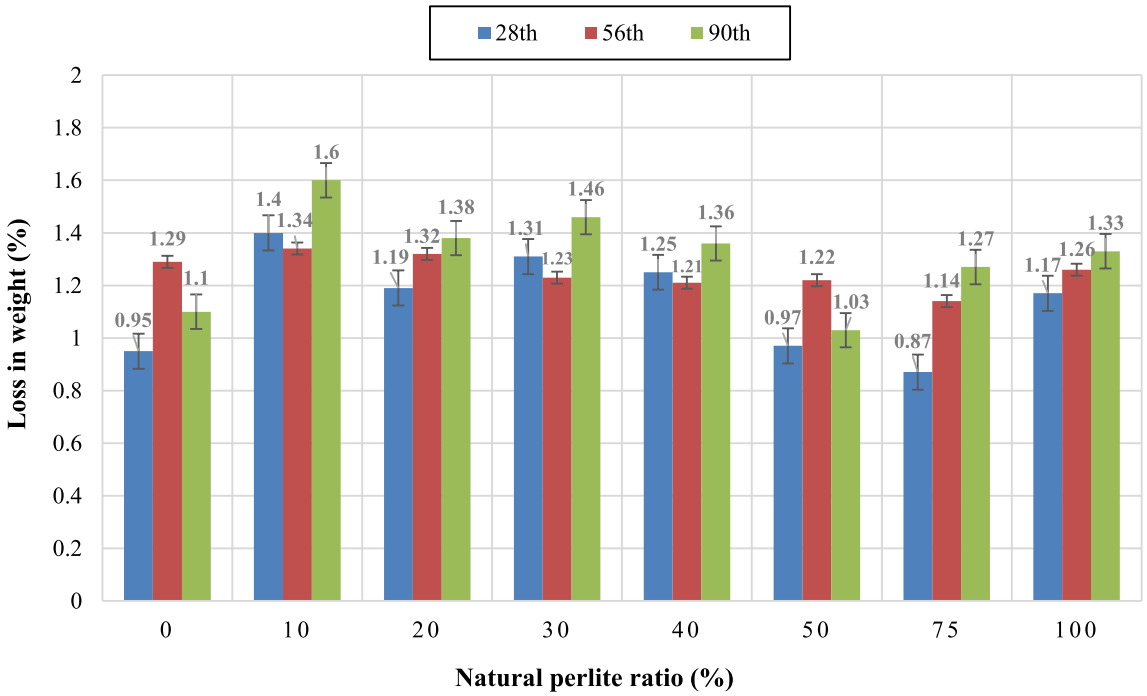

Fig. 18 Loss in weight of sulfate attacked concretes

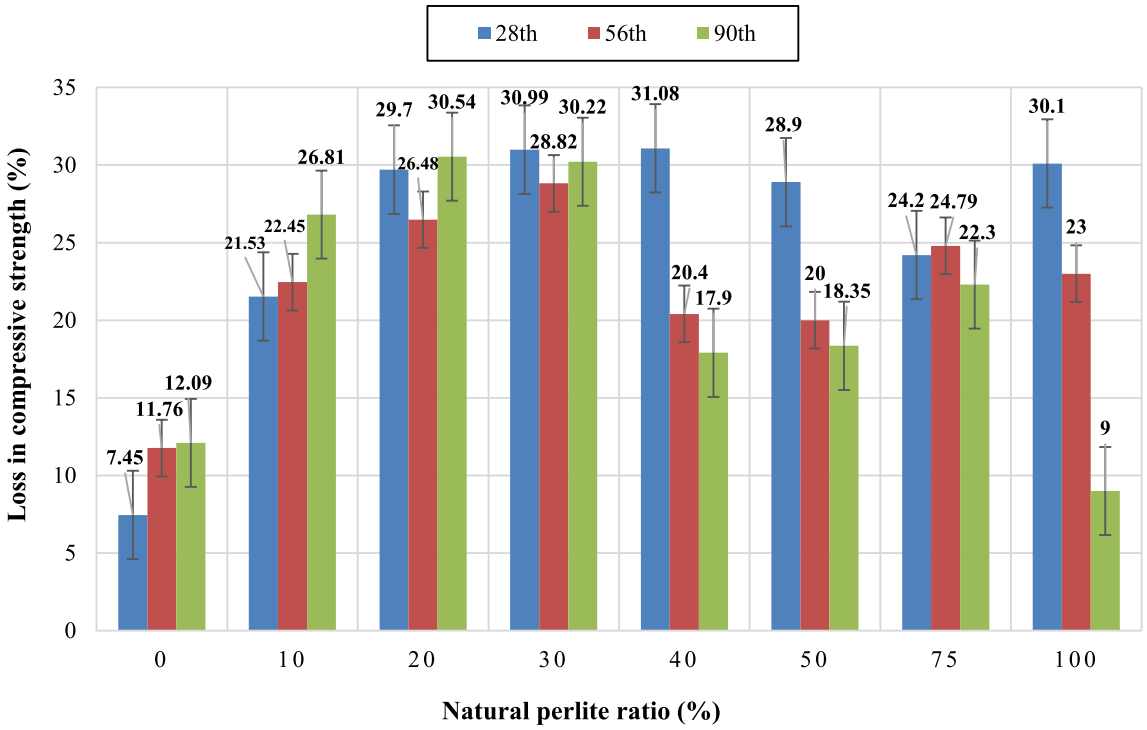

Fig. 19 Loss in compressive strength of sulfate attacked concretes

natural perlite increases due to the effect of sulfate, the small weight losses observed in this study demonstrated that when natural perlite is used as an aggregate in concrete, concretes with high sulfate resistance can be produced. Similar observations were obtained in very few studies in the literature (Kasaniya et al. 2021).

3.8.2 Compressive strength loss of sulfate attacked concretes

The compressive strength losses of concrete exposed to sulfate solution for 28, 56, and 90 days are presented in Fig. 19.

After 28 days of sulfate attack, the concretes' compressive strength losses increased with the natural perlite ratio increasing from 0 to 40%. While the compressive strength loss of the control concrete was 7.45%, the loss of the concrete produced with 30% natural perlite was 30.99%, which was about four times higher. Losses in compressive strength were almost at the same level with the increase in the proportion of natural perlite up to 100%. The results at 56 and 90 days were similar; the compressive strength losses were highest in concrete with 30% natural perlite and decreased as the natural perlite content increased. The high resistance of concretes produced using natural perlite against sulfate attack with advanced age is believed to increase the resistance against sulfate ion penetration by forming a refined and curved pore network due to the additional cemented hydrated formation as a result of the consumption of calcium hydroxide, which is vulnerable to sulfate attack, by perlite, which is a natural pozzolan, through pozzolanic reaction (Kaid et al. 2009; Carsana et al. 2014). Similar to the acid attack results, it was determined that the 30% natural perlite ratio was the critical ratio in the sulfate attack results. The concretes with this ratio showed less resistance to aggressive solutions.

Finally, the visual results of the specimens after the sulfate attack were evaluated through Figs. 20 and 21. Figure 20 shows that regardless of the natural perlite ratio, the specimens similarly deteriorated to a lesser extent, in parallel with the results of weight loss due to sulfate attack.

Figure 21 illustrates that as the sulfate exposure period progressed (from 28 to 90 days), the concrete deteriorated more. However, the least deterioration occurred in control and 100% natural perlite concrete, while the most deterioration occurred in the concrete with 30% natural perlite, which can be clearly detected as peeling on the surface and capping of the aggregates, and results were confirmed by the visual results.

As stated in recent reviews of lightweight aggregate concretes (Leong et al. 2020; Chinnu et al. 2021), studies to determine the ability of these concrete to withstand aggressive environments are almost non-existent, and more research is necessary. In this context, with this study, the behavior of lightweight aggregate concretes composed

Fig. 20 Images of concrete exposed to sulfate attack for 28 days. Concretes containing 0%, 30% and 100% natural perlite

Fig. 21 Images of concrete exposed to sulfate attack for 90 days. Concretes containing 0%, 30% and 100% natural perlite

of natural perlite against acid and sulfate attack has been investigated for the first time and introduced to the scientific literature.

4 Conclusion

As a result of this study in which the mechanical, permeability, and durability properties of lightweight concrete composites produced with different proportions of natural perlite were investigated; especially the utilization of increasing proportions of natural perlite resulted in a decrease in fresh density values. As the concrete age increased, the lightweight concrete produced using 10% natural perlite reached the highest compressive strength value among all groups (62.42 MPa for NP10/90). This study also revealed that high strength lightweight concrete (50 MPa and above) can be produced using 10% natural perlite. The UPV test results proved that lightweight concretes produced with natural perlite can be classified as good or excellent concretes. The dynamic modulus of elasticity values of the concretes decreased sharply when the natural perlite content increased to 50% and above for all days. The capillary water absorption coefficients of the concretes increased by up to 67% as the natural perlite content increased. Electrical resistivity test results unearthed that 40% natural perlite content is the critical threshold. It was observed that insulating concretes can be produced by increasing the utilization rate of natural perlite at advanced ages (the electrical resistivity value of concrete with 100% natural perlite (139.75 kΩ-m for NP100/90) is 140% higher than the control concrete (58.14 kΩ-m for C/90). It was determined that concretes with 75% and 100% natural perlite exhibited high resistance against acid and sulfate attack, while 30% perlite ratio was the critical ratio and concretes with this ratio exhibited less resistance against acid and sulfate solution.

The high resistance of lightweight concrete composites with natural perlite aggregates, especially against electrical resistivity, acid and sulfate attack, has been introduced to the literature for the first time in this study. In addition, for the purpose of this study, it has been proved that lightweight concretes with high natural perlite dosage can be produced in terms of permeability and durability properties without compromising mechanical strength. In terms of sustainability, it is believed that the superior engineering properties of lightweight concrete composites with natural perlite aggregate for the production of a more environmentally friendly concrete with less destruction of natural resources are promising for future studies.

Author contributions HAB was responsible to design experimental setup, perform laboratory works, data acquisition, and write manuscript. The manuscript has been read and approved by all named author.

Funding No funding was available for the present study.

Data availability The raw/processed data required to reproduce these findings cannot be shared at this time as the data also form as part of an ongoing study.

Declarations

Conflict of interest The author states that he has no conflicting interests to declare.

Ethical approval This article does not contain any studies with human participants or animals performed by any of the authors.

Human or animal rights No conflicts, informed consent, human or animal rights are applicable to this study.

References

Abdul Ajeej K, Varun Teja K, Meena T (2019) Experimental study on mechanical properties and micro-structure of perlite powder concrete subjected to elevated temperatures. Int J Recent Technol Eng 7(6):1350–1357

Adhikary SK, Ashish DK, Sharma H, Patel J, Rudžionis Ž, Al-Ajamee M, Thomas BS, Khatib JM (2022) Lightweight self-compacting concrete: a review. Resour Conserv Recycl Adv 15:200107. https://doi.org/10.1016/j.rcradv.2022.200107

Aghabeyk F, Azadmehr A, Hezarkhani A (2022) Fabrication of feldspar-based geopolymers from perlite toward decontamination of heavy metals from aqueous solution: hydrolysis process, characterizations, kinetic and isotherm studies. J Environ Chem Eng 10(4):108087. https://doi.org/10.1016/j.jece.2022.108087

Akyuncu V, Sanliturk F (2021) Investigation of physical and mechanical properties of mortars produced by polymer coated perlite aggregate. J Build Eng 38:102182. https://doi.org/10.1016/j.jobe.2021.102182

Arrigoni A, Panesar DK, Duhamel M, Opher T, Saxe S, Posen ID, MacLean HL (2020) Life cycle greenhouse gas emissions of concrete containing supplementary cementitious materials: cut-off vs. substitution. J Clean Prod 263:121465. https://doi.org/10.1016/j.jclepro.2020.121465

Ashtiani R, Saeed A, Hammons M (2014) Mechanistic characterization and performance evaluation of recycled aggregate systems. J Mater Civ Eng 26(1):99–106. https://doi.org/10.1061/(ASCE)MT.1943-5533.0000798

Aslam M, Shafigh P, Jumaat MZ (2016) Oil-palm by-products as lightweight aggregate in concrete mixture: a review. J Clean Prod 126:56–73. https://doi.org/10.1016/j.jclepro.2016.03.100

ASTM C1012 (2019) Standard test method for length change of hydraulic-cement mortars exposed to a sulfate solution. ASTM International, West Conshohocken, PA, USA

ASTM C1585 (2020) Standard test method for measurement of rate of absorption of water by hydraulic-cement concretes. ASTM International, West Conshohocken, PA, USA

ASTM C1760 (2012) Standard test method for bulk electrical conductivity of hardened concrete. ASTM International, West Conshohocken, PA, USA

ASTM C267 (2020) Standard test methods for chemical resistance of mortars, grouts, and monolithic surfacings and polymer concretes. ASTM International, West Conshohocken, PA, USA

ASTM C597 (2016) Standard test method for pulse velocity through concrete. ASTM International, West Conshohocken, PA, USA

ASTM C618 (2023) Standard specification for coal ash and raw or calcined natural pozzolan for use in concrete. ASTM International, West Conshohocken, PA, USA

Barnat-Hunek D, Grzegorczyk-Frańczak M, Klimek B, Pavlíková M, Pavlík Z (2021) Properties of multi-layer renders with fly ash and boiler slag admixtures for salt-laden masonry. Constr Build Mater 278:122366. https://doi.org/10.1016/j.conbuildmat.2021.122366

Baskar I, Prabavathy S, Jeyasubramanian K, Anuradha R, Awoyera PO (2022) Thermal and mechanical characterization of microencapsulated phase change material in cementitious composites. Iran J Sci Technol Transact Civ Eng 46(2):1141–1151. https://doi.org/10.1007/s40996-021-00636-5

Burbano-Garcia C, Hurtado A, Silva YF, Delvasto S, Araya-Letelier G (2021) Utilization of waste engine oil for expanded clay aggregate production and assessment of its influence on lightweight concrete properties. Constr Build Mater 273:121677. https://doi.org/10.1016/j.conbuildmat.2020.121677

Carsana M, Frassoni M, Bertolini L (2014) Comparison of ground waste glass with other supplementary cementitious materials. Cement Concr Compos 45:39–45. https://doi.org/10.1016/j.cemconcomp.2013.09.005

Chihaoui R, Siad H, Senhadji Y, Mouli M, Nefoussi AM, Lachemi M (2022) Efficiency of natural pozzolan and natural perlite in controlling the alkali-silica reaction of cementitious materials. Case Stud Constr Mater 17:e01246. https://doi.org/10.1016/j.cscm.2022.e01246

Chinchillas-Chinchillas MJ, Orozco-Carmona VM, Gaxiola A, Alvarado-Beltrán CG, Pellegrini-Cervantes MJ, Baldenebro-López FJ, Castro-Beltrán A (2019) Evaluation of the mechanical properties, durability and drying shrinkage of the mortar reinforced with polyacrylonitrile microfibers. Constr Build Mater 210:32–39. https://doi.org/10.1016/j.conbuildmat.2019.03.178

Chinnu SN, Minnu SN, Bahurudeen A, Senthilkumar R (2021) Reuse of industrial and agricultural by-products as pozzolan and aggregates in lightweight concrete. Constr Build Mater 302:124172. https://doi.org/10.1016/j.conbuildmat.2021.124172

Demirboğa R, Gül R (2003) Thermal conductivity and compressive strength of expanded perlite aggregate concrete with mineral admixtures. Energy Build 35(11):1155–1159. https://doi.org/10.1016/j.enbuild.2003.09.002

Demirboğa R, Örüng İ, Gül R (2001) Effects of expanded perlite aggregate and mineral admixtures on the compressive strength of low-density concretes. Cem Concr Res 31(11):1627–1632. https://doi.org/10.1016/S0008-8846(01)00615-9

Diamanti MV, Brenna A, Bolzoni F, Berra M, Pastore T, Ormellese M (2013) Effect of polymer modified cementitious coatings on water and chloride permeability in concrete. Constr Build Mater 49:720–728. https://doi.org/10.1016/j.conbuildmat.2013.08.050

Erdem TK, Meral Ç, Tokyay M, Erdoğan TY (2007) Use of perlite as a pozzolanic addition in producing blended cements. Cement Concr Compos 29(1):13–21. https://doi.org/10.1016/j.cemconcomp.2006.07.018

Esfandiari J, Heidari O (2021) Investigation on the behavior of concrete with optimum percentage of steel fiber, microsilica, fly ash and hybrid fiber under different loading pattern. J Struct Constr Eng 8(6):130–150. https://doi.org/10.22065/JSCE.2020.182908.1840

Esfandiari J, Loghmani P (2019) Effect of perlite powder and silica fume on the compressive strength and microstructural characterization of self-compacting concrete with lime-cement binder. Measurement 147:106846. https://doi.org/10.1016/j.measurement.2019.07.074

Gencel O, Bayraktar OY, Kaplan G, Arslan O, Nodehi M, Benli A, Gholampour A, Ozbakkaloglu T (2022) Lightweight foam concrete containing expanded perlite and glass sand: physico-mechanical, durability, and insulation properties. Constr Build Mater 320:126187. https://doi.org/10.1016/j.conbuildmat.2021.126187

Guenanou F, Khelafi H, Aattache A (2019) Behavior of perlite-based mortars on physicochemical characteristics, mechanical and carbonation: case of perlite of Hammam Boughrara. J Build Eng 24:100734. https://doi.org/10.1016/j.jobe.2019.100734

Hanif A, Lu Z, Cheng Y, Diao S, Li Z (2017) Effects of different lightweight functional fillers for use in cementitious composites. Int J Concr Struct Mater 11:99–113. https://doi.org/10.1007/s40069-016-0184-1

Huang G, Pudasainee D, Gupta R, Liu WV (2021) Thermal properties of calcium sulfoaluminate cement-based mortars incorporated with expanded perlite cured at cold temperatures. Constr Build Mater 274:122082. https://doi.org/10.1016/j.conbuildmat.2020.122082

IS 13311 (1992) Part 1, non-destructive testing of concrete: methods of test—ultrasonic pulse velocity. Indian Standard

Işıkdağ B (2015) Characterization of lightweight ferrocement panels containing expanded perlite-based mortar. Constr Build Mater 81:15–23. https://doi.org/10.1016/j.conbuildmat.2015.02.009

Jia G, Li Z (2021) Influence of the aerogel/expanded perlite composite as thermal insulation aggregate on the cement-based materials: preparation, property, and microstructure. Constr Build Mater 273:121728. https://doi.org/10.1016/j.conbuildmat.2020.121728

Junaid MF, Rehman Z, Kuruc M, Medveď I, Bačinskas D, Čurpek J, Čekon M, Ijaz N, Ansari WS (2022) Lightweight concrete from a perspective of sustainable reuse of waste byproducts. Constr Build Mater 319:126061. https://doi.org/10.1016/j.conbuildmat.2021.126061

Kaid N, Cyr M, Julien S, Khelafi H (2009) Durability of concrete containing a natural pozzolan as defined by a performance-based approach. Constr Build Mater 23(12):3457–3467. https://doi.org/10.1016/j.conbuildmat.2009.08.002

Kalpana M, Tayu A (2020) Experimental investigation on lightweight concrete added with industrial waste (steel waste). Mater Today Proc 22(3):887–889. https://doi.org/10.1016/j.matpr.2019.11.096

Karakaş H, İlkentapar S, Durak U, Örklemez E, Özuzun S, Karahan O, Atiş CD (2023) Properties of fly ash-based lightweight-geopolymer mortars containing perlite aggregates: mechanical, microstructure, and thermal conductivity coefficient. Constr Build Mater 362:129717. https://doi.org/10.1016/j.conbuildmat.2022.129717

Karein SMM, Vosoughi P, Isapour S, Karakouzian M (2018) Pretreatment of natural perlite powder by further milling to use as a supplementary cementitious material. Constr Build Mater 186:782–789. https://doi.org/10.1016/j.conbuildmat.2018.08.012

Kasaniya M, Thomas MDA, Moffatt EG (2021) Efficiency of natural pozzolans, ground glasses and coal bottom ashes in mitigating sulfate attack and alkali-silica reaction. Cement Concr Res 149:106551. https://doi.org/10.1016/j.cemconres.2021.106551

Kotwica Ł, Pichór W, Kapeluszna E, Różycka A (2017) Utilization of waste expanded perlite as new effective supplementary cementitious material. J Clean Prod 140(Part 3):1344–1352. https://doi.org/10.1016/j.jclepro.2016.10.018

Krausmann F, Gingrich S, Eisenmenger N, Erb KH, Haberl H, Fischer-Kowalski M (2009) Growth in global materials use, GDP and population during the 20th century. Ecol Econ 68(10):2696–2705. https://doi.org/10.1016/j.ecolecon.2009.05.007

Lanzón M, García-Ruiz PA (2008) Lightweight cement mortars: advantages and inconveniences of expanded perlite and its influence on fresh and hardened state and durability. Constr Build Mater 22(8):1798–1806. https://doi.org/10.1016/j.conbuildmat.2007.05.006

Leong GW, Mo KH, Loh ZP, Ibrahim Z (2020) Mechanical properties and drying shrinkage of lightweight cementitious composite incorporating perlite microspheres and polypropylene fibers. Constr Build Mater 246:118410. https://doi.org/10.1016/j.conbuildmat.2020.118410

Li N, Zhang S, Long G, Jin Z, Yu Y, Zhang X, Xiong C, Li H (2021) Dynamic characteristics of lightweight aggregate self-compacting concrete by impact resonance method. Adv Civ Eng 2021:8811303. https://doi.org/10.1155/2021/8811303

Marie I (2016) Zones of weakness of rubberized concrete behavior using the UPV. J Clean Prod 116:217–222. https://doi.org/10.1016/j.jclepro.2015.12.096

Mir AE, Nehme SG (2017) Utilization of industrial waste perlite powder in self-compacting concrete. J Clean Prod 156:507–517. https://doi.org/10.1016/j.jclepro.2017.04.103

Oktay H, Yumrutaş R, Akpolat A (2015) Mechanical and thermophysical properties of lightweight aggregate concretes. Constr Build Mater 96:217–225. https://doi.org/10.1016/j.conbuildmat.2015.08.015

Ortiz O, Castells F, Sonnemann G (2009) Sustainability in the construction industry: a review of recent developments based on LCA. Constr Build Mater 23(1):28–39. https://doi.org/10.1016/j.conbuildmat.2007.11.012

Othman ML, Alsarayreh AIM, Abdullah R, Sarbini NN, Yassin MS, Ahmad H (2020) Experimental study on lightweight concrete using lightweight expanded clay aggregate (LECA) and expanded perlite aggregate (EPA). J Eng Sci Technol 15(2):1186–1201. https://doi.org/10.6084/m9.figshare.12253481

Pasupathy K, Ramakrishnan S, Sanjayan J (2022) Enhancing the properties of foam concrete 3D printing using porous aggregates. Cement Concr Compos 133:104687. https://doi.org/10.1016/j.cemconcomp.2022.104687

Polat BY (2022) Self healing of alkali active mortars with expanded perlite aggregate. Case Stud Constr Mater 17:e01225. https://doi.org/10.1016/j.cscm.2022.e01225

Ragul P, Hari MNT, Arunachelam N, Chellapandian M (2022) An experimental study on the partial replacement of fine aggregate with perlite in cement concrete. Mater Today Proc 68(5):1219–1224. https://doi.org/10.1016/j.matpr.2022.05.578

Ramezanianpour AA, Karein SMM, Vosoughi P, Pilvar A, Isapour S, Moodi F (2014) Effects of calcined perlite powder as a SCM on the strength and permeability of concrete. Constr Build Mater 66:222–228. https://doi.org/10.1016/j.conbuildmat.2014.05.086

Rao SK, Sravana P, Chandrasekhara Rao T (2016) Experimental studies in ultrasonic pulse velocity of roller compacted concrete pavement containing fly ash and M-sand. Int J Pavement Res Technol 9(4):289–301. https://doi.org/10.1016/j.ijprt.2016.08.003

Rashad AM (2016) A synopsis about perlite as building material-a best practice guide for civil engineer. Constr Build Mater 121:338–353. https://doi.org/10.1016/j.conbuildmat.2016.06.001

Różycka A, Pichór W (2016) Effect of perlite waste addition on the properties of autoclaved aerated concrete. Constr Build Mater 120:65–71. https://doi.org/10.1016/j.conbuildmat.2016.05.019

Sahoo S, Selvaraju AK, Prakash SS (2020) Mechanical characterization of structural lightweight aggregate concrete made with sintered fly ash aggregates and synthetic fibres. Cement Concr Compos 113:103712. https://doi.org/10.1016/j.cemconcomp.2020.103712

Sayadi A, Neitzert TR, Clifton GC (2018) Influence of poly-lactic acid on the properties of perlite concrete. Constr Build Mater 189:660–675. https://doi.org/10.1016/j.conbuildmat.2018.09.029

Schumacher K, Saßmannshausen N, Pritzel C, Trettin R (2020) Lightweight aggregate concrete with an open structure and a porous matrix with an improved ratio of compressive strength to dry density. Constr Build Mater 264:120167. https://doi.org/10.1016/j.conbuildmat.2020.120167

Sengul O, Azizi S, Karaosmanoglu F, Tasdemir MA (2011) Effect of expanded perlite on the mechanical properties and thermal conductivity of lightweight concrete. Energy Build 43(2–3):671–676. https://doi.org/10.1016/j.enbuild.2010.11.008

Siwowski T, Rajchel M (2019) Structural performance of a hybrid FRP composite–lightweight concrete bridge girder. Compos Part B Eng 174:107055. https://doi.org/10.1016/j.compositesb.2019.107055

Snellings R (2016) Assessing, understanding and unlocking supplementary cementitious materials. RILEM Tech Lett 1:50

Swamy RN, Tanikawa S (1993) An external surface coating to protect concrete and steel from aggressive environments. Mater Struct 26:465–478. https://doi.org/10.1007/BF02472806

Thomaz WA, Miyaji DY, Possan E (2021) Comparative study of dynamic and static young's modulus of concrete containing basaltic aggregates. Case Stud Constr Mater 15:e00645. https://doi.org/10.1016/j.cscm.2021.e00645

Top S, Vapur H, Altiner M, Kaya D, Ekicibil A (2020) Properties of fly ash-based lightweight geopolymer concrete prepared using pumice and expanded perlite as aggregates. J Mol Struct 1202:127236. https://doi.org/10.1016/j.molstruc.2019.127236

Topçu İB, Işıkdağ B (2007) Manufacture of high heat conductivity resistant clay bricks containing perlite. Build Environ 42(10):3540–3546. https://doi.org/10.1016/j.buildenv.2006.10.016

Topçu İB, Işıkdağ B (2008) Effect of expanded perlite aggregate on the properties of lightweight concrete. J Mater Process Technol 204(1–3):34–38. https://doi.org/10.1016/j.jmatprotec.2007.10.052

Topçu İB, Uygunoğlu T (2010) Effect of aggregate type on properties of hardened self-consolidating lightweight concrete (SCLC). Constr Build Mater 24(7):1286–1295. https://doi.org/10.1016/j.conbuildmat.2009.12.007

Torres ML, García-Ruiz PA (2009) Lightweight pozzolanic materials used in mortars: evaluation of their influence on density, mechanical strength and water absorption. Cement Concr Compos 31(2):114–119. https://doi.org/10.1016/j.cemconcomp.2008.11.003

TS En 12350–6 (2019) Testing fresh concrete—part 6: density. Turkish Standards Institution, Ankara, Turkey (Turkish Codes)

TS En 12390–3 (2019) Testing hardened concrete—part 3: compressive strength of test specimens. Turkish Standards Institution, Ankara, Turkey (Turkish Codes)

Urhan S (1987) Alkali silica and pozzolanic reactions in concrete. part 2: observations on expanded perlite aggregate concretes. Cement Concr Res 17(3):465–477. https://doi.org/10.1016/0008-8846(87)90010-X

van Jaarsveld JGS, van Deventer JSJ (1999) Effect of the alkali metal activator on the properties of fly ash-based geopolymers. Ind Eng Chem Res 38(10):3932–3941. https://doi.org/10.1021/ie980804b

Wang X, Wu D, Hou D, Yu R, Geng Q, Wang P, Wang M, Zhang C, Li L, Li X (2022) The unification of light weight and ultra-high strength in LWC: a new homogeneity enhancement approach. Constr Build Mater 315:125647. https://doi.org/10.1016/j.conbuildmat.2021.125647

Yu LH, Ou H, Lee LL (2003) Investigation on pozzolanic effect of perlite powder in concrete. Cem Concr Res 33(1):73–76. https://doi.org/10.1016/S0008-8846(02)00924-9

Yu R, van Onna DV, Spiesz P, Yu QL, Brouwers HJH (2016) Development of ultra-lightweight fibre reinforced concrete applying

expanded waste glass. J Clean Prod 112(Part1):690–701. https://doi.org/10.1016/j.jclepro.2015.07.082

Zhang Z, Provis JL, Reid A, Wang H (2015) Mechanical, thermal insulation, thermal resistance and acoustic absorption properties of geopolymer foam concrete. Cement Concr Compos 62:97–105. https://doi.org/10.1016/j.cemconcomp.2015.03.013

Zhang Z, Provis JL, Zou J, Reid A, Wang H (2016) Toward an indexing approach to evaluate fly ashes for geopolymer manufacture. Cem Concr Res 85:163–173. https://doi.org/10.1016/j.cemconres.2016.04.007

Zhao X, Hwang B, Lim J (2020) Job satisfaction of project managers in green construction projects: constituents, barriers, and improvement strategies. J Clean Prod 246:118968. https://doi.org/10.1016/j.jclepro.2019.118968